



## Novel rare earth (Ce and La) hydrotalcite like material: Synthesis and characterization

E. Rodrigues<sup>a,\*</sup>, P. Pereira<sup>b</sup>, T. Martins<sup>b</sup>, F. Vargas<sup>b</sup>, T. Scheller<sup>c</sup>, J. Correa<sup>c</sup>, J. Del Nero<sup>d</sup>, S.G.C. Moreira<sup>d</sup>, W. Ertel-Ingrisch<sup>e</sup>, C.P. De Campos<sup>e</sup>, A. Gigler<sup>e</sup>

<sup>a</sup> Faculdade de Química, ICEN, Universidade Federal do Pará, 66075-110 Belém, PA, Brazil

<sup>b</sup> Faculdade de Química, GD, Brazil

<sup>c</sup> Faculdade de Geologia, IG, Brazil

<sup>d</sup> Faculdade de Física, ICEN, Brazil

<sup>e</sup> LMU, Department für Geo- und Umweltwissenschaften, München, Germany

### ARTICLE INFO

#### Article history:

Received 20 April 2011

Accepted 10 March 2012

Available online 23 March 2012

#### Keywords:

REE HT compounds

Cerium

Lanthanum

MgAlLaO solid solution

ultrasonic homogenization

### ABSTRACT

Novel rare earth element hydrotalcite-like compounds (REE HT) also referred as layered double hydroxides were produced by co-precipitation with ultrasound homogenization under low supersaturation condition. Thermal treatment was performed at 500 °C and 650 °C. Samples were characterized by several methods: X-Ray Diffraction (XRD), Fourier Transformed Infrared Spectroscopy (FTIR), Raman Spectroscopy (RS), Scanning Electron Microscopy (SEM) and Electron Microprobe (EMP). The assemblage data obtained, increasing on cell parameters and the hexagonal symmetry confirmed the partial substitution of Al<sup>3+</sup> by Ce<sup>3+</sup> and La<sup>3+</sup> in the HT structure. La HT is an effective precursor for MgAlLaO solid solution of MgO-type materials, being very promising to be several catalytic applications.

© 2012 Elsevier B.V. All rights reserved.

### 1. Introduction

The structure of layered double hydroxide (LDH) or hydrotalcite (HT), expressed by the general formula  $[M^{2+}_{1-x}M^{3+}_x(OH)_2]^{x+}(A^{n-}_{x/n})^x \cdot mH_2O$ , consists of layers with M<sup>2+</sup> cations partially replaced by M<sup>3+</sup> cations. Excess positive charge is compensated by interlayer anions (A<sup>n-</sup> = e.g., CO<sub>3</sub><sup>2-</sup>, NO<sub>3</sub><sup>-</sup>, Cl<sup>-</sup>, etc.) located in the hydrated inter-layer region [1,2]. A wide range of possible cations and anions that could be incorporated in the HT structure gives rise to several different materials. Catalytic activities on these compounds are related to surface and textural properties like particle size, surface area, size distributions, and pore shapes. Basic HT properties are mainly determined by inter-layer cations, M<sup>2+</sup>/M<sup>3+</sup> ratio, compensation anions, and activation parameters [3,4]. Several HT compounds have been synthesized with different preparation methods. Co-precipitation, at constant or variable pH, over a range of temperatures, is the most common procedure [5–7]. Thermal decomposition of HT at mild temperatures produces small crystals sized, mixed oxides with high specific superficial areas, high stability under thermal treatment, and a wide variability of active sites. These oxides can be used as drug derivatives, catalysts, supported ionic catalyst changers and metal adsorbents [8,9]. These REE mixed and simple oxides are related to basic sites [14]. Allied to their

distinctive electronic and magnetic properties, applications of the REE in high-technology and environmental purposes have grown dramatically in diversity and importance over the past four decades [10].

The main focus of this work is the partial incorporating (50%) of Ce<sup>3+</sup> and La<sup>3+</sup> by Al<sup>3+</sup> in the Mg/Al–CO<sub>3</sub> structure system in order to produce REE HT compounds to be used as convenient precursors for mixed oxides.

### 2. Materials and methods

#### 2.1. Starting materials

Two starting compositions  $[Mg_6AlX(CO_3)(OH)_{16}4H_2O]$  (X = Ce or La) for Cerium and Lanthanum were synthesized according to co-precipitation procedures with a homogenization step performed in an ultrasonic bath at 48 °C. Mg, Al, Ce, and La were introduced in form of nitrates. Nitrate solutions were added to an aqueous solution of NaOH / Na<sub>2</sub>CO<sub>3</sub> while stirring was applied. Starting slurry was then aged for 24 h and washed several times with purified water at a constant pH value of = 10. Solutions were dried at 100 °C for 12 h and submitted to a thermal treatment at two different temperatures (500 °C and 650 °C) by over 2 h in a muffle furnace. The temperature conditions were chosen based on previous work calcinations at high temperature decomposes the hydrotalcite and well-dispersed mixed Mg–Al,Ce,La oxides which presents sites that are associated to structural hydroxyl groups [11–19].

\* Corresponding author. Fax: +55 9132017966.

E-mail address: [beth@ufpa.br](mailto:beth@ufpa.br) (E. Rodrigues).

## 2.2. Characterization

In order to understand and correlate data of morphological, textural, chemical and spectroscopic studies several techniques were employed SEM were performed with a on a Zeiss - LEO 1430 microscope, operated at 25 kV and 40 mA current. XRD patterns were collected at room temperature in an XPERT-PRO/PW3050 diffractometer, using Cu K $\alpha$  radiation ( $\lambda = 1.54056 \text{ \AA}$ ), with 40 kV, 40 mA, 2 deg/min from  $2\theta = 5^\circ$  to  $70^\circ$ , and 20 s. Lattice parameters and lattice volume were calculated from a least-squares method using the (0 0 3), (0 0 6), (1 1 0), and (1 1 3) reflections for HT; and using the (2 0 0) and (2 2 0) reflections for MgAlLaO mixed oxide type materials.

Calculation of apparent crystallite size (D) for HT and MgAlLaO mixed oxide type powders has been performed by Debye-Scherrer formula [ $\beta(2\theta) = 0.94\lambda / (D \cos \theta_0)$ ], using (0 0 3) and (1 1 0) reflections for HT and the (2 0 0) reflection for MgAlLaO mixed oxide type materials, employing the FWHM procedure.

EMP were carried out with a Cameca SX-100, operated at 15 kV, 20 mA, and 1  $\mu\text{m}$ . Raman spectroscopy were performed with a WITec  $\alpha$ -300R using a 532 nm laser. FTIR were carried out on Thermal Electron Corporation / IR 100 equipment, in a 4000 to 400  $\text{cm}^{-1}$  range.

Along the text samples will be denoted: Ce HT and La HT for the unheated samples; Ce HT 500 and La HT 500 for samples heated at 500  $^\circ\text{C}$  and Ce HT 650 and La HT 650 for samples heated at 650  $^\circ\text{C}$ .

## 3. Results and discussion

A set of SEM images is shown in Fig. 1, showed a Ce HT sample presented crystal size and crystallinity higher than La HT (Fig. 1a). La HT agglomerates are up to 50 times bigger ( $\sim 100 \mu\text{m}$ ) than the corresponding single small sized crystallites ( $\sim 2 \mu\text{m}$ ) (Fig. 1b). The presence of a cubic  $\text{CeO}_2$  phase has also been observed (Fig. 1c). Those samples presented a small increase in crystal size ( $\sim 3 \mu\text{m}$ ) in comparison to the Ce HT sample.

Powder X-ray diffraction patterns of rare earth HT materials are showed in Fig. 2. Unheated samples presented a layered structure,

typical of materials type hydrotalcite. Oxide, hydroxide and carbonate phases were also detected in these samples. For Ce HT sample,  $\text{CeO}_2$  and  $\text{Ce}_2\text{O}(\text{CO}_3)_2\text{H}_2\text{O}$  were recorded while for the La HT sample,  $\text{La}(\text{OH})_3$  and  $\text{LaCO}_3\text{OH}$  were observed (Table 1). Strong anionic character of Lanthanum favored formation of carbonate species in very early stages of co-precipitation and in corroboration with its high ionic radius [13] prevented intercalation of larger lanthanum species in HT galleries.

Major peaks of REE HT indexed [(0 0 3), (0 0 6), (0 1 2), (0 0 9), (0 1 5), (0 1 8), (1 1 0), and (1 1 3)] presented a shift position toward left in comparison to positions observed on HT (Table 1). Crystallochemical parameters reported in literature for Mg/Al- $\text{CO}_3$  HT [5–7,12] are lower than these presented for our REE HT samples. Lattice parameters ( $a = b 3.09$  and  $c = 24.31 \text{ \AA}$  – Ce HT) ( $a = b 3.10$  and  $c = 24.40 \text{ \AA}$ ) also led to an enlargement of interlayer distances and a substitution on sheets as consequence of large effective ionic radius of Ce (1,01  $\text{ \AA}$ ) and La (1,03  $\text{ \AA}$ ) in comparison with Al (0,54  $\text{ \AA}$ ) [13]. As reported in literature, HT modified with REE in an amount of approximately amount of approximately 10% (w/w) ( $\text{Mg}_{0.75}\text{Al}_{0.23}\text{La}_{0.02}\text{-HT}$ ) [14] presents lattice parameters close to HT (Table 1), however this is only valid for very low REE insertion into HT structure (but the insertion of REE into the HT structure is very low).

The few number of peaks was determined the lattice parameters and the symmetry indexed as hexagonal. From those four peaks lattice parameters were determined (Table 1). Crystallite size also presented higher values than reported in literature for HT, evidencing a deformation of HT structure. Measurements of (0 0 3) reflections indicated values for crystallite thickness of 79  $\text{ \AA}$  (10.93 $^\circ$ ) and 91  $\text{ \AA}$  (10.87 $^\circ$ ) for Ce HT and La HT, respectively. Further (1 1 0) reflections indicated values for Ce HT and La HT crystallite diameters of 124  $\text{ \AA}$  (59.97 $^\circ$ ) and 280  $\text{ \AA}$  (60.72 $^\circ$ ), respectively (Table 1).

Heat treatment, at 500  $^\circ\text{C}$  and 650  $^\circ\text{C}$ , provided an improvement on intensity and resolution of XRD data from calcinated HT samples (Fig. 2). Layered structure collapses of Ce HT 500 and Ce HT 650 samples, leading to an assemblage of simple oxides:  $\text{CeO}_2$  and MgO (Table 1). Despite heating temperature, for as La HT samples, structure of HT-like minerals was preserved. Characteristic diffraction peaks (0 0 3), (0 0 6), (1 1 0) and (1 1 3) were registered at both heating

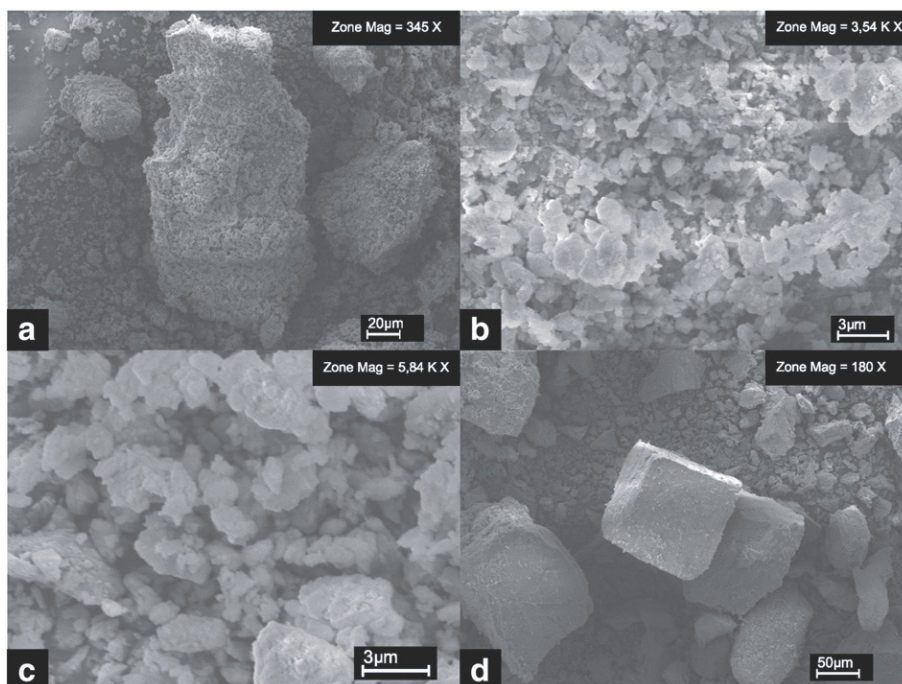
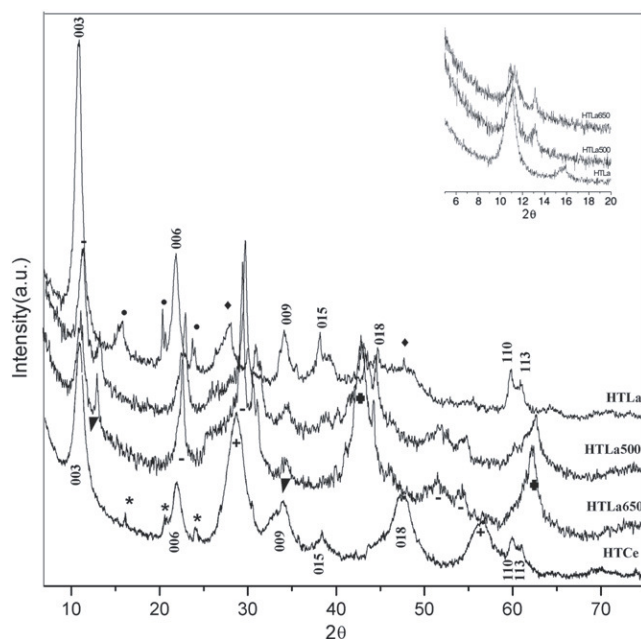


Fig. 1. SEM micrographs of Ce HT and La HT samples.



**Fig. 2.** XRD patterns of REE HT samples a) Ce HT (\*  $\text{Ce}_2\text{O}(\text{CO}_3)_2\text{H}_2\text{O}$ , +  $\text{CeO}_2$ ); b) La HT (●  $\text{LaCO}_3\text{OH}$ , ◆  $\text{La}(\text{OH})_3$ ); c) La HT 500; d) La HT 650 (♣  $\text{Mg}(\text{Al}^{3+}/\text{La}^{3+})\text{O}$ , ▼  $\text{La}_2\text{O}_2\text{CO}_3$ , —  $\text{La}_2(\text{CO}_3)_3\cdot 8\text{H}_2\text{O}$ ).

temperature mineral assemblages observed for La HT were,  $\text{La}_2\text{O}_2\text{CO}_3$  and  $\text{MgAlLaO}$  mixed oxide non-type materials.  $\text{MgO}$ -type  $\text{MgAlLaO}$  solid solution has already been reported in literature [14,15].

Previously lattice parameters and crystallite size are quite similar to the values obtained in this work (Table 1). Presence of  $\text{La}_2\text{O}_2\text{CO}_3$  was attributed to contamination by air during sample manipulation. XRD data of Ce and La HT samples are characteristic of hydrotalcite-like structural phase. Low supersaturation conditions ( $\text{pH}=10$ ) seem to lead to a more disordered HT structure as appropriate to accommodate REE species

EMP data showed that large ions could be introduced in HT structure. Metal chemical composition of samples Ce HT and La HT indicated a nominal metal ratio  $\text{M}^{2+}/\text{M}^{3+}$  slightly below the expected value of 3 (Table 1). Heat treatment affected atomic proportions of all metal cations on HT structure; heated samples (La HT 500 and La HT 650) exhibited a  $\text{M}^{2+}/\text{M}^{3+}$  ratio slightly above 3.

Assignment of peaks in Raman spectra of REE HT samples exhibited a behavior similar to HT structures described in literature [5,7,20,21] (Fig. 3). Ce HT presented a broad vibration centered at  $3460\text{ cm}^{-1}$  and a peak at  $3695\text{ cm}^{-1}$ , that are vibrations due to OH stretching of sorbed water. Stretching modes at  $1357\text{ cm}^{-1}$ ,  $1046/1084\text{ cm}^{-1}$  and  $604/720\text{ cm}^{-1}$  attributed respectively to a  $\nu_3\text{ CO}_3^{2-}$ ,  $\nu_1\text{ CO}_3^{2-}$  and  $\nu_4\text{ CO}_3^{2-}$ .  $\text{Mg}/\text{Al}$ -OH translation modes were observed at  $461/546\text{ cm}^{-1}$ .

La HT vibrations due to OH stretching of sorbed water result in a broad vibration centered at  $3500\text{ cm}^{-1}$  and a peak at  $3700\text{ cm}^{-1}$ . For

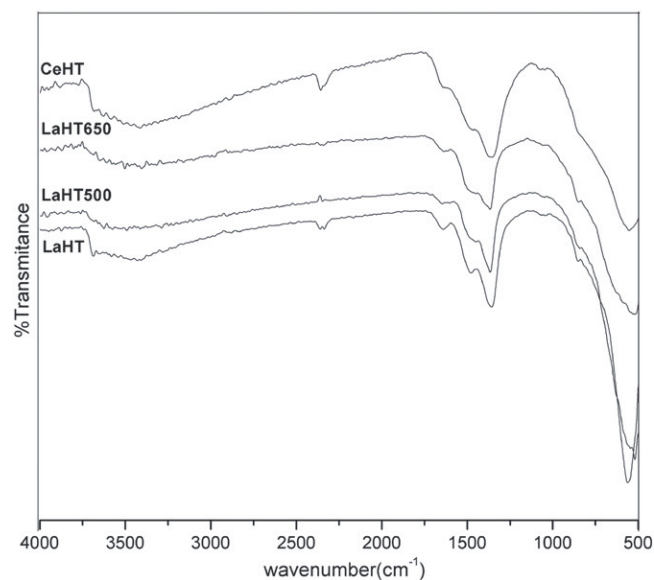
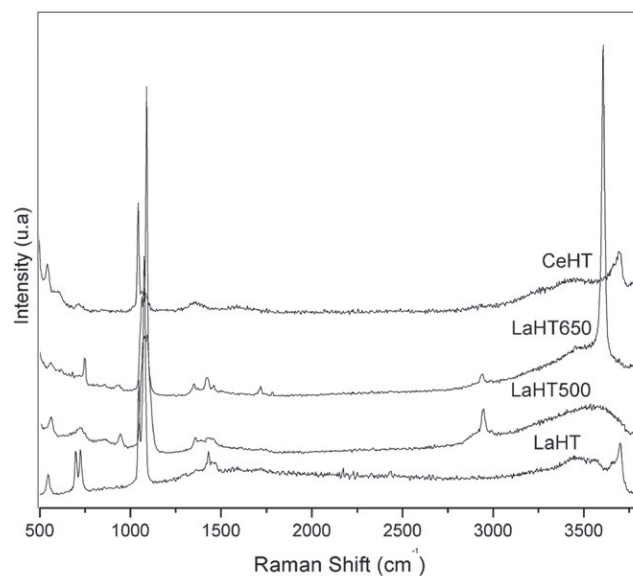


**Fig. 3.** Raman spectra and FTIR spectra of REE LDH samples: a) Ce HT; b) La HT; c) La HT 500; d) La HT 650.

La HT 500 same vibrations were firstly observed at  $2940\text{ cm}^{-1}$ , followed by a broad vibration centered at  $3500\text{ cm}^{-1}$  and a peak at  $3713\text{ cm}^{-1}$ . Background of signal changed for La HT 650, beginning at  $2900\text{ cm}^{-1}$ , followed by a broad vibration centered at  $3460\text{ cm}^{-1}$  and a peak at  $3605\text{ cm}^{-1}$ .  $\nu_3\text{ CO}_3^{2-}$  stretching modes were recorded at  $1430/1470\text{ cm}^{-1}$  for La HT, at  $1352/1421\text{ cm}^{-1}$  for La HT 500 and at  $1350/1421/1460\text{ cm}^{-1}$  for La HT 650.  $\nu_1\text{ CO}_3^{2-}$  stretching mode was recorded

**Table 1**

Metal chemical compositions (in atomic proportions), nominal metal ratio ( $\text{M}^{2+}/\text{M}^{3+}$ ) and lattice parameters of material (change name table).

Samples	Lattice parameters	c (Å)	Lattice parameters	V (Å <sup>3</sup> )	D (Å)	2θ – hkl	$\text{M}^{2+}/\text{M}^{3+}$ ratio
	a = b (Å)		a = b = c (Å)				
$\text{Mg}_{7.28}\text{Al}_{1.52}\text{Ce}_{1.19}$ at%	$3.0399 \pm 0.0024$	$24.3715 \pm 0.0528$	–	$195 \pm 0.254$	79	10.93 (003)	2.70
$\text{Mg}_{7.46}\text{Al}_{1.68}\text{La}_{0.86}$ at%	$3.1027 \pm 0.0011$	$24.3754 \pm 0.0233$	–	$203.2 \pm 0.234$	98	10.86 (003)	2.94
La HT500	$3.0798 \pm 0.0007$	$23.7598 \pm 0.0135$	–	$195.2 \pm 0.140$	–	–	3.18
La HT650	$3.0304 \pm 0.0034$	$23.4167 \pm 0.0683$	–	$186.2 \pm 0.687$	–	–	3.12
$\text{Mg}_{0.75}\text{Al}_{0.23}\text{La}_{0.02}\text{HT}$ [14]	3.07	23.68	–	–	–	–	–
$\text{Mg}_{0.76}\text{Al}_{0.185}\text{Ce}_{0.055}\text{HDT}$ [15]	3.08	24.02	–	–	–	–	–
OxidoHT5*	–	–	4.20	74.09	34	46.06 (200)	–
OxidoHT65	–	–	4.16	73.56	32	43.13 (200)	–
$\text{Mg}(\text{Al})\text{LaO}$ [14]	–	–	4.18	73.03	30.5	43 (200)	–

at 1046/1084  $\text{cm}^{-1}$  for La HT, at 1062/1070/1084  $\text{cm}^{-1}$  for La HT 500 and at 1063/1088  $\text{cm}^{-1}$  for La HT 650. Al–OH translation mode was observed at 935  $\text{cm}^{-1}$  for both La HT 500 and La HT 650. La HT did not reveal a peak related to this mode.  $\nu_4 \text{CO}_3^{2-}$  stretching mode was recorded at 697/723  $\text{cm}^{-1}$  for La HT, at 715  $\text{cm}^{-1}$  for La HT 500 and at 745  $\text{cm}^{-1}$  for La HT 650.  $\nu_2 \text{CO}_3^{2-}$  stretching mode was recorded at 546  $\text{cm}^{-1}$ , 555  $\text{cm}^{-1}$ , 559  $\text{cm}^{-1}$ , for La HT, La HT 500, and La HT 650, respectively. Mg/Al–OH translation modes were observed at 470/483  $\text{cm}^{-1}$  for La HT, at 461/480  $\text{cm}^{-1}$  for La HT 500 and at 447/461  $\text{cm}^{-1}$  for La HT 650.

All REE HT samples exhibited similar FTIR spectra and were also very similar to hydrotalcite [20–22] and hydrotalcite-like compounds containing cerium [15] (Fig. 3). Ce HT presented a broad vibration centered at 3407  $\text{cm}^{-1}$  due to OH stretching of adsorbed water. Bending mode of water was recorded at 1640  $\text{cm}^{-1}$ . Vibration at 1355  $\text{cm}^{-1}$  is attributed to  $\nu_3 \text{CO}_3^{2-}$  stretching mode, at 1049  $\text{cm}^{-1}$  to  $\nu_1 \text{CO}_3^{2-}$  stretching mode, 830  $\text{cm}^{-1}$  to  $\nu_2 \text{CO}_3^{2-}$  stretching mode. Mg/Al–OH translation modes were observed at 549  $\text{cm}^{-1}$ .

For La HT, OH stretching of sorbed water was observed as a broad peak centered at 3374  $\text{cm}^{-1}$ . This peak was shifted to 3492  $\text{cm}^{-1}$  and 3600  $\text{cm}^{-1}$  for La HT 500 and La HT 650, respectively.  $\nu_3 \text{CO}_3^{2-}$  stretching mode were recorded at 1359/1477  $\text{cm}^{-1}$  for La HT, at 1365/1452  $\text{cm}^{-1}$  for La HT 500 and at 1367/1490  $\text{cm}^{-1}$  for La HT 650.  $\nu_1 \text{CO}_3^{2-}$  stretching mode was recorded at 1060  $\text{cm}^{-1}$  for La HT, while it was shifted to 1070  $\text{cm}^{-1}$  for La HT 500 and in La HT 650.  $\nu_2 \text{CO}_3^{2-}$  stretching mode was recorded at 850  $\text{cm}^{-1}$  for La HT, La HT 500, and La HT 650 samples. Mg/Al–OH translation modes were observed at 651  $\text{cm}^{-1}$  for La HT, 522  $\text{cm}^{-1}$  for La HT 500 and 518  $\text{cm}^{-1}$  for La HT 650.

#### 4. Conclusions

The thermal decomposition of REE HT based on a ratio  $\text{M}^{2+}/\text{M}^{3+} = 3$  (Mg/Al + X, X = Ce or La) with carbonate in interlayer region synthesized by co-precipitation with ultrasonic homogenization was studied and characterized by several complementary techniques: XRD, FTIR, Raman, SEM and EMP.

The crystallization of the REE HT was confirmed by hydroxyl groups, interlayer anions and the octahedral lattice. The products of thermal decomposition are quite different on REE HT samples. La HT ( $\text{Mg}_{7.46}\text{Al}_{1.68}\text{La}_{0.86}$  at%) was an effective precursor to MgAlLaO mixed oxide type materials, but Ce HT ( $\text{Mg}_{7.28}\text{Al}_{1.52}\text{Ce}_{1.19}$  at%) submitted to the same thermal conditions produced single oxides (MgO and  $\text{CeO}_2$ ). The mixed oxide formed by thermal decomposition of La HT is a non stoichiometric mixture and exhibited a very small crystal size ( $\sim 30$  Å).

#### Acknowledgments

The authors are grateful to Prof. Lamarão and Prof. Angélica for their support on SEM images acquisition and XRD data. We also thank

Dr. Robert Stark for the Raman data. CAPES/DAAD provided the financial support for this work.

#### References

- [1] Kovanda F, Rojka T, Dobesova J, Machovic V, Bezdicka P, Obalova L, et al. Mixed oxides obtained from Co and Mn containing layered double hydroxides: preparation, characterization and catalytic properties. *J Solid State Chem* 2006;179:812–23.
- [2] Cavani F, Trifiro F, Vaccari A. Hydrotalcite-type anionic clays: preparation, properties and applications. *Catal Today* 1991;11:173–301.
- [3] Xie Wenlei, Peng Hong, Chen L. Calcined Mg–Al hydrotalcites as solid base catalysts for methanolysis of soybean oil. *J Mol Catal A* 2006;246:24–32.
- [4] Cantrell DG, Gillie LJ, Lee AF, Wilson K. Structure–reactivity correlations in MgAl hydrotalcite catalysts for biodiesel synthesis. *Appl Catal* 2005;287:183–90.
- [5] Rives V. Layered double hydroxides: present and future. 2nd ed. New York: Nova science publishers; 2001.
- [6] Duan X, Evans DG. Double hydroxides (structure and bonding). Berlin: Springer-Verlag; 2006. xrd ed.
- [7] Braterman PS, Xu ZP, Yarberry F. Layered double hydroxides (LDHs). In: Auerbach SM, Carrado KAE, Dutta PK, editors. *Handbook of Layered Materials*. New York: Marcel Dekker Inc.; 2004. p. 373–474.
- [8] Diez VK, Apestguia CR, Di Cosimo JL. Effect of the chemical composition on the catalytic performance of MgAlOx catalysts for alcohol elimination reactions. *J Catal* 2003;215:215–20.
- [9] Kannan S, Dube A, Knozinger H. Synthesis and characterization of CuMgAl ternary hydrotalcites as catalysts for the hydroxylation of phenol. *J Catal* 2005;231:381–92.
- [10] Angelescu E, Pavel OD, Che M, Birjega R, Constantin G. Cyanoethylation of ethanol on Mg–Al hydrotalcites promoted by  $\text{Y}^{3+}$  and  $\text{La}^{3+}$ . *Catal Commun* 2004;5:647–51.
- [11] Reichle WT. Catalytic reactions by thermally activated, synthetic, anionic clay-minerals. *J Catal* 1985;94:547–57.
- [12] Pu M, Zhang B. Theoretical study on the microstructures of hydrotalcite lamellae with Mg/Al ratio of two. *Mater Lett* 2005;59:3343–7.
- [13] Shu X, Zhang W, He J, Gao F, Zhu Y. Formation of Ni–Ti-layered double hydroxides using homogenous precipitation method. *Solid State Sci* 2006;8:634–9.
- [14] Birjega R, Pavel OD, Constantin G, Angelescu E. Rare-earth elements modified hydrotalcites and corresponding mesoporous mixed oxides as basic solid catalysts. *Appl Catal A* 2005;288:185–93.
- [15] Das J, Das D, Parida KM. Preparation and characterization of Mg–Al hydrotalcite-like compounds containing cerium. *J Colloid Interface Sci* 2006;301:569–74.
- [16] Zhao D, Yang Q, Han Z, Sun F, Tang K, Yu F. Rare earth hydroxycarbonate materials with Hierarchical structures: preparation and characterization and catalytic activity of derived oxides. *Solid State Sci* 2008;10:1028–36.
- [17] Zhu J, Yuan P, He H, Frost L, Tao Q, Shen W, et al. in situ synthesis of surfactant/silane-modified hydrotalcites. *J Colloid Interface Sci* 2008;319:498–504.
- [18] Kandare E, Hossenlopp J. Thermal degradation of acetate-intercalated hydroxy double and layered hydroxy salts. *Inorg Chem* 2006;45:3766–73.
- [19] Ma R, Liu Z, Takada K, Lyi N, Bando Y, Sasaki T. Synthesis and exfoliation of  $\text{Co}^{2+}$ – $\text{Fe}^{3+}$  layered double hydroxides: an innovative topochemical approach; 2007. *Jacs Article*.
- [20] Frost L, Erickson K. Raman spectroscopic study of the hydrotalcite desautelsite  $\text{Mg}_6\text{Mn}_2\text{CO}_3(\text{OH})_{16}\cdot 4\text{H}_2\text{O}$ . *Spectrochim Acta Part A* 2005;11:2697–701.
- [21] Tsyganok A, Sayari A. Incorporation of transition metals into Mg–Al layered double hydroxides: coprecipitation of cations vs. their pre-complexation with an anionic chelator. *J Solid State Chem* 2006;179:1830–41.
- [22] Klopogge T, Wharton D, Hickey L, Frost RL. Infrared and Raman study of interlayer anions  $\text{CO}_3^{2-}$ ,  $\text{NO}_3^-$ ,  $\text{SO}_4^{2-}$  and  $\text{ClO}_4^-$  in Mg/Al hydrotalcite. *Am Mineral* 2002;87:623–7.